THE BELL SYSTEM TECHNICAL JOURNAL
Vol. 52, No. 3, March, 1973
Printed in U.S.A.

Tube Waveguide for Optical Transmission

By D. MARCUSE and W. L. MAMMEL

(Manuscript received September 25, 1972)

The dielectric optical waveguide described in this paper has an annular cross section, the refractive index of which is higher than the indices of the material inside and outside of the ring. The solution of the eigenvalue problem is an approximation which is valid for small refractive index differences of the three media. The resulting approximate eigenvalue equation is far simpler than its exact counterpart. The cutoff conditions of the first three modes and the eigenvalue of the lowest-order mode are presented graphically.

I. INTRODUCTION

Dielectric optical waveguides have become interesting since it has been demonstrated that the losses of dielectric materials can be quite low.[1–3] The conventional optical fiber waveguide consists of a solid dielectric core surrounded by a dielectric material with lower refractive index. This structure has the advantage of being particularly simple. In this paper we analyze a different type of dielectric optical waveguide. Our structure consists of a dielectric tube which is filled and surrounded by dielectric material with lower index of refraction. Such structures have been analyzed before.[4] A complete discussion of and references to the literature can be found in Ref. 5. However, the exact analytical treatment is extremely complicated so that the resulting theories are hard to apply to practical situations. Recently A. W. Snyder[6] has shown that the analysis of the conventional optical fiber waveguide becomes much simpler if one assumes that the difference of the refractive indices of core and cladding material is only slight. D. Gloge[7] has developed Snyder's theoretical work even further. On the basis of this simplified method of analysis, it is possible to treat rather complicated optical waveguide structures more simply and still obtain results that are applicable to most cases of practical interest. The simplification that results from the assumption of only slight index

differences is particularly appropriate since most practical dielectric optical waveguides satisfy this requirement.

An approximate eigenvalue equation for the modes of the tube waveguide and an equation describing the cutoff conditions for these modes are derived in this paper. The connection of the tube waveguide with the dielectric slab waveguide in the limit of large tube radii and with the solid-core optical fiber in the limit of small tube radii is discussed. The cutoff condition for the first three modes is represented graphically and the eigenvalue of the first mode is plotted.

For simplicity we assume throughout that the index of the material inside of the tube is smaller than or equal to the index of the material surrounding the tube.

II. APPROXIMATE MODE ANALYSIS OF THE TUBE WAVEGUIDE

The geometry of the tube waveguide is shown in Fig. 1. Following the ideas of Snyder and Gloge[6,7] we express the electric and magnetic field components in rectangular cartesian coordinates and write[8]

$$E_x = -\frac{i}{K_j^2}\left(\beta\frac{\partial E_z}{\partial x} + \omega\mu\frac{\partial H_z}{\partial y}\right) \tag{1}$$

$$E_y = -\frac{i}{K_j^2}\left(\beta\frac{\partial E_z}{\partial y} - \omega\mu\frac{\partial H_z}{\partial x}\right) \tag{2}$$

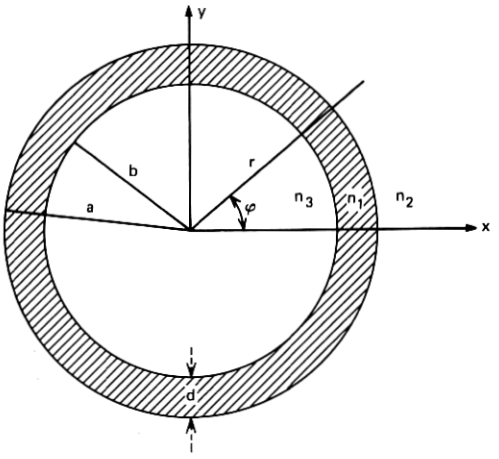

Fig. 1—Cross section of the tube waveguide.

$$H_x = -\frac{i}{K_j^2}\left(\beta\frac{\partial H_z}{\partial x} - \omega\epsilon\frac{\partial E_z}{\partial y}\right) \tag{3}$$

$$H_y = -\frac{i}{K_j^2}\left(\beta\frac{\partial H_z}{\partial y} + \omega\epsilon\frac{\partial E_z}{\partial x}\right). \tag{4}$$

It is assumed that the time and z dependence of the field are determined by the factor

$$e^{i(\omega t-\beta z)}. \tag{5}$$

β is the propagation constant in z direction, ω is the radian frequency. The parameter K_j is defined as

$$K_j^2 = n_j^2k^2 - \beta^2 \qquad j = 1, 2, \text{ or } 3 \tag{6}$$

with

$$k^2 = \omega^2\epsilon_o\mu_o. \tag{7}$$

Equations (1) through (4) are exact and are simply four of Maxwell's six equations written in a different form. If the refractive indices are all nearly the same, $n_1 \approx n_2 \approx n_3 \approx n$, we must have

$$\beta \approx nk, \tag{8}$$

so that

$$K_j \ll \beta. \tag{9}$$

It is thus apparent that the transverse field components are much larger than the longitudinal components if the refractive indices are all very nearly the same. The longitudinal field components are obtained as solutions of the wave equations.[8] We use the expressions

$$E_z = \frac{iA_jK_j}{2n_jk}\{Z_{\nu+1}(K_jr)\sin(\nu+1)\phi + Z_{\nu-1}(K_jr)\sin(\nu-1)\phi\} \tag{10}$$

$$H_z = -\sqrt{\frac{\epsilon_o}{\mu_o}}\frac{iA_jK_j}{2k}\{Z_{\nu+1}(K_jr)\cos(\nu+1)\phi - Z_{\nu-1}(K_jr)\cos(\nu-1)\phi\}. \tag{11}$$

The exponential factor (5) has been suppressed. $Z_\nu(K_jr)$ is a cylinder function and A_j is an arbitrary amplitude factor. Substitution of (10) and (11) into (1) through (4) results in

$$E_y = A_jZ_\nu(K_jr)\cos\nu\phi, \tag{12}$$

$$H_x = -n_jA_j\sqrt{\frac{\epsilon_o}{\mu_o}}Z_\nu(K_jr)\cos\nu\phi, \tag{13}$$

and

$$E_x = 0, \qquad H_y = 0. \tag{14}$$

These equations are approximations that hold provided that (8) is applicable.

In the three regions shown in Fig. 1, we use the following cylinder functions and parameters, assuming $n_1 > n_2 > n_3$,

$$\left.\begin{aligned} -iK_3 &= \theta = (\beta^2 - n_3^2k^2)^{\frac{1}{2}} \\ Z_\nu &= J_\nu(i\theta r) \end{aligned}\right\} \quad \text{for} \quad 0 \leqq r \leqq b \tag{15}$$

$$\left.\begin{aligned} K_1 &= \kappa = (n_1^2k^2 - \beta^2)^{\frac{1}{2}} \\ Z_\nu &= J_\nu(\kappa r) + BN_\nu(\kappa r) \end{aligned}\right\} \quad \text{for} \quad b \leqq r \leqq a \tag{16}$$

$$\left.\begin{aligned} -iK_2 &= \gamma = (\beta^2 - n_2^2k^2)^{\frac{1}{2}} \\ Z_\nu &= H_\nu^{(1)}(i\gamma r) \end{aligned}\right\} \quad \text{for} \quad a \leqq r \leqq \infty. \tag{17}$$

J_ν, N_ν are the Bessel and Neumann functions and $H_\nu^{(1)}$ is the Hankel function of the first kind. We use the functions with imaginary argu-

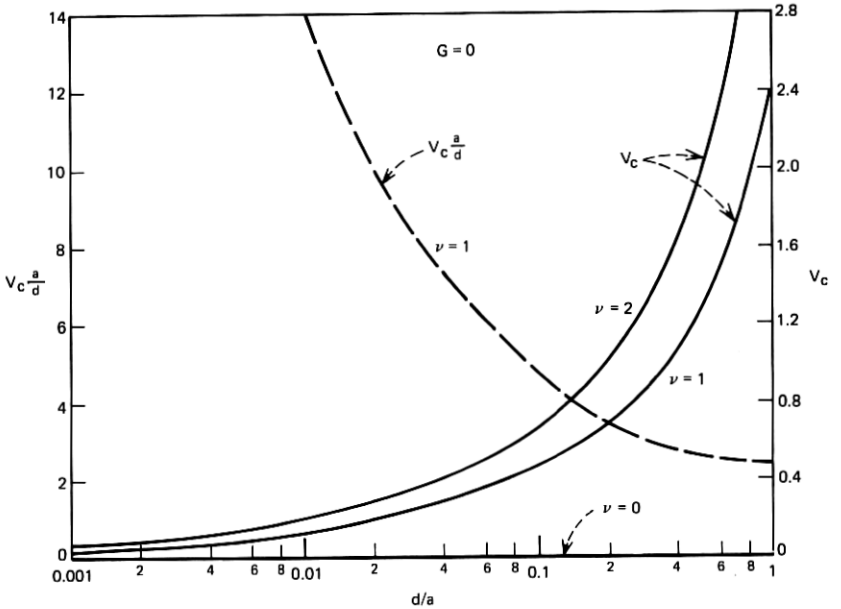

Fig. 2—The cutoff value of the normalized frequency V for $G = 0$ as a function of the ratio of wall thickness d to tube (outer) radius a. The cutoff value for the mode $\nu = 0$ is $V = 0$.

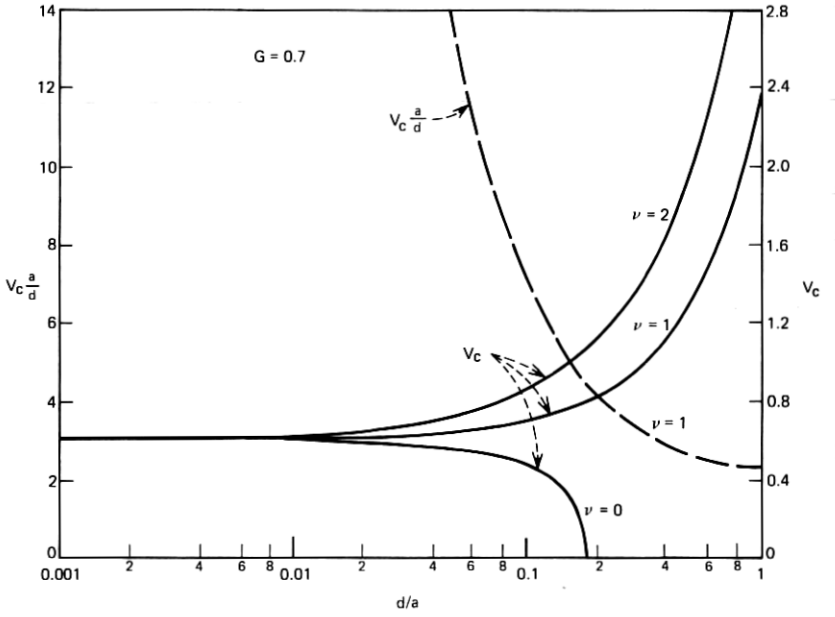

Fig. 3—The cutoff value of V as a function of d/a for $G = 0.7$.

ments instead of modified functions. This practice is in agreement with Jahnke and Emde[9] as well as with Gradshteyn and Ryzhik.[10] The amplitude coefficient A_j appearing in (10) through (13) also assumes different values in the three regions of space, $j = 1, 2, 3$.

In order to be able to match the boundary conditions, we transform the cartesian components to vector components in cylindrical polar coordinates

$$E_\phi = -E_x \sin \phi + E_y \cos \phi$$
$$= \tfrac{1}{2} A_j Z_\nu(K_j r)[\cos(\nu + 1)\phi + \cos(\nu - 1)\phi] \quad (18)$$

$$H_\phi = \tfrac{1}{2} n_j A_j \sqrt{\frac{\epsilon_o}{\mu_o}} Z_\nu(K_j r)[\sin(\nu + 1)\phi - \sin(\nu - 1)\phi]. \quad (19)$$

The boundary conditions require that E_z, E_ϕ, H_z, and H_ϕ are continuous at $r = b$ and at $r = a$. The boundary conditions thus provide us with eight equations. However, our approximate treatment of the modes yields only four arbitrary constants, A_1, A_2, A_3, and B. The situation is further aggravated if we observe that the field components contain the functions $\sin(\nu + 1)\phi$ and $\sin(\nu - 1)\phi$ and corresponding

expressions with the cosine function. Since the boundary conditions must hold for all values of ϕ, we must equate the coefficients of the functions with $\nu + 1$ independently of those with $\nu - 1$, thus doubling the number of equations. In spite of this apparently hopeless situation, approximate solutions are possible. The equations that result from the requirement that the tangential components of **E** are continuous at the boundaries differ from the corresponding equations resulting from the boundary conditions for **H** only by factors n_j. Since our approach is based on assuming that all n_j are nearly the same, we set these factors all equal to the same average value n and, after dividing by n, obtain equations that duplicate those obtained from the boundary conditions for **E**. To the approximation considered here, the **E** and **H** boundary conditions lead to the same set of equations, reducing their total number to one half of the original number. To satisfy the continuity of E_z and E_ϕ at $r = b$, we equate the coefficients of $\sin(\nu + 1)\phi$ and obtain

$$A_3 = \frac{J_\nu(\kappa b) + BN_\nu(\kappa b)}{J_\nu(i\theta b)} A_1 \tag{20}$$

and the determinantal condition

$$i\theta \frac{J_{\nu+1}(i\theta b)}{J_\nu(i\theta b)} = \kappa \frac{J_{\nu+1}(\kappa b) + BN_{\nu+1}(\kappa b)}{J_\nu(\kappa b) + BN_\nu(\kappa b)}. \tag{21}$$

Equating the coefficients of $\sin(\nu - 1)\phi$, we obtain a similar result with the only difference that $\nu + 1$ is replaced by $\nu - 1$ in (21). Equation (20) remains the same. With the help of the recursion relations[9,10] for cylinder functions, it is easy to prove that eq. (21) is not changed if $\nu + 1$ is replaced by $\nu - 1$. We thus find ourselves in the happy position of being able to satisfy–at least approximately–the eight boundary conditions at $r = b$ with the two available coefficients. In an analogous fashion, we obtain from the boundary conditions at $r = a$ the equation

$$A_2 = \frac{J_\nu(\kappa a) + BN_\nu(\kappa a)}{H_\nu^{(1)}(i\gamma a)} A_1 \tag{22}$$

and the determinantal condition

$$i\gamma \frac{H_{\nu+1}^{(1)}(i\gamma a)}{H_\nu^{(1)}(i\gamma a)} = \kappa \frac{J_{\nu+1}(\kappa a) + BN_{\nu+1}(\kappa a)}{J_\nu(\kappa a) + BN_\nu(\kappa a)}. \tag{23}$$

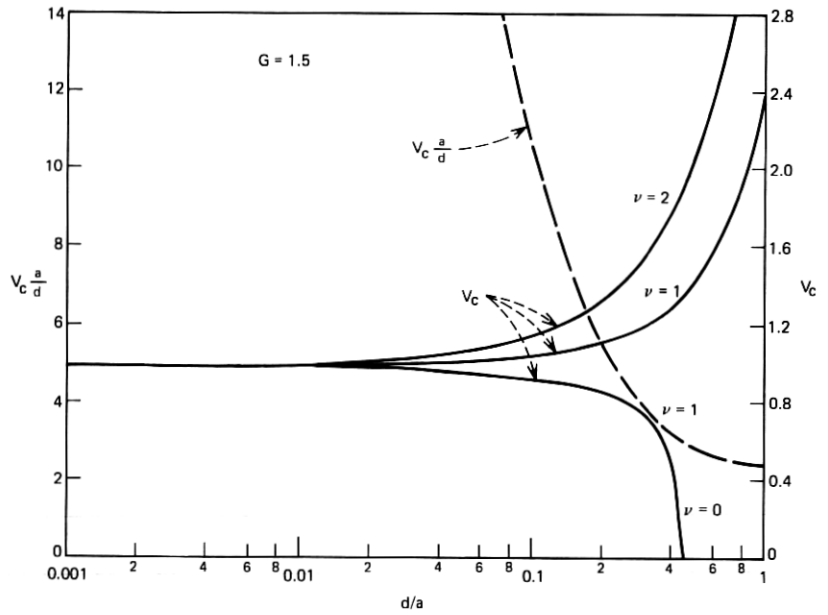

Fig. 4—Same as Fig. 3, $G = 1.5$.

The eigenvalue equation is obtained by eliminating B from (21) and (23). We find

$$\frac{\kappa J_\nu(i\theta b)J_{\nu+1}(\kappa b) - i\theta J_\nu(\kappa b)J_{\nu+1}(i\theta b)}{\kappa J_\nu(i\theta b)N_{\nu+1}(\kappa b) - i\theta N_\nu(\kappa b)J_{\nu+1}(i\theta b)} = \frac{\kappa H_\nu^{(1)}(i\gamma a)J_{\nu+1}(\kappa a) - i\gamma J_\nu(\kappa a)H_{\nu+1}^{(1)}(i\gamma a)}{\kappa H_\nu^{(1)}(i\gamma a)N_{\nu+1}(\kappa a) - i\gamma N_\nu(\kappa a)H_{\nu+1}^{(1)}(i\gamma a)}. \quad (24)$$

The constant B is given by

$$B = -\frac{\kappa J_\nu(i\theta b)J_{\nu+1}(\kappa b) - i\theta J_\nu(\kappa b)J_{\nu+1}(i\theta b)}{\kappa J_\nu(i\theta b)N_{\nu+1}(\kappa b) - i\theta N_\nu(\kappa b)J_{\nu+1}(i\theta b)}. \quad (25)$$

It can be shown that the eigenvalue equation (24) specializes to the eigenvalue equation ($d = a - b$)

$$\tan \kappa d = \frac{\kappa(\gamma + \theta)}{\kappa^2 - \gamma\theta} \quad (26)$$

of the asymmetric slab waveguide in the limit $a \to \infty$ and $b \to \infty$. The

distinction between TE and TM modes of the slab waveguide is lost in our approximation.

We are mainly interested in the cutoff conditions of the modes in order to find the separation between the lowest and the next higher mode which determines the range of single-mode operation. Cutoff is defined by the condition

$$\gamma = 0. \tag{27}$$

In order to determine the cutoff frequency, we use (27) in (24) and obtain the cutoff equation

$$\frac{J_\nu\left(iGV\frac{b}{d}\right)J_{\nu+1}\left(V\frac{b}{d}\right) - iGJ_\nu\left(V\frac{b}{d}\right)J_{\nu+1}\left(iGV\frac{b}{d}\right)}{J_\nu\left(iGV\frac{b}{d}\right)N_{\nu+1}\left(V\frac{b}{d}\right) - iGN_\nu\left(V\frac{b}{d}\right)J_{\nu+1}\left(iGV\frac{b}{d}\right)} = \frac{J_{\nu-1}\left(V\frac{a}{d}\right)}{N_{\nu-1}\left(V\frac{a}{d}\right)}. \tag{28}$$

The parameters appearing in this equation are defined as follows:

$$V = (n_1^2 - n_2^2)^{\frac{1}{2}}kd \tag{29}$$

and

$$G = \left(\frac{n_2^2 - n_3^2}{n_1^2 - n_2^2}\right)^{\frac{1}{2}}. \tag{30}$$

For future reference, we derive an interesting relation for the mode with $\nu = 0$. The cutoff condition (28) allows the solution $V = 0$ for $\nu = 0$. We find as the condition that $V = 0$, the relation

$$\frac{d}{a} = 1 - \left(\frac{n_1^2 - n_2^2}{n_1^2 - n_3^2}\right)^{\frac{1}{2}} = 1 - \frac{1}{(1 + G^2)^{\frac{1}{2}}}. \tag{31}$$

In the limit of infinite radii, $a \to \infty$ and $b \to \infty$, we obtain from (26) the cutoff condition for $n_1 > n_2 \geqq n_3$

$$V = \arctan G. \tag{32}$$

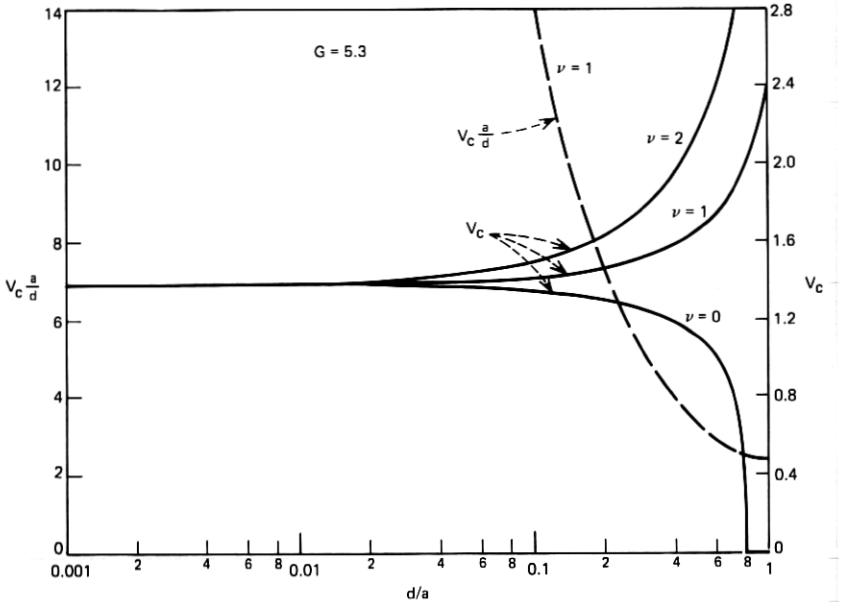

Fig. 5—Same as Fig. 3, $G = 5.3$.

III. DISCUSSION AND NUMERICAL RESULTS

We restrict our discussion to the case $n_2 \geqq n_3$. The cutoff values of V [see eq. (29)] as functions of d/a are plotted in Figs. 2 through 6 as solid lines for the first three modes, $\nu = 0$, $\nu = 1$, $\nu = 2$. The V parameter characterizes the tube waveguide in the limit of large radii where it can be regarded as an asymmetric slab waveguide that is bent into a circle. For large values of d/a, the waveguide approaches an optical fiber with solid cylindrical core. Such a fiber is characterized by a different V parameter which can be expressed in our notation as $(a/d)V$. In the limit $d/a = 1$, both parameters coincide. The parameter $(a/d)V$ is plotted in the figures as a dotted line only for the mode $\nu = 1$. Each curve, Figs. 2 through 6, is plotted for a different value of G [see eq. (30)]. The relation between the G values and the ratios of n_1/n_2 and n_1/n_3 is shown in Fig. 7.

Since the tube waveguide approaches the asymmetric slab in the limit $d/a = 0$ and the solid-core fiber in the limit $d/a = 1$, the cutoff values $V = V_c$ can be predicted at these limits. For $d/a = 1$, the cutoff value of the solid-core fiber is obtained from

$$J_{\nu-1}(V_c) = 0. \tag{33}$$

The values of V_c at $d/a = 1$ are, therefore, $V_c = 0$ for $\nu = 0$, $V_c = 2.405$ for $\nu = 1$, and $V_c = 3.83$ for $\nu = 2$.

At $d/a = 0$, we find the cutoff values for V from the asymmetric slab formula (32).

We see from Figs. 3 through 6 that the curve with $\nu = 0$ seems to end on the horizontal axis. Actually, the curve must be continued along the horizontal axis at $V = 0$ to the point $d/a = 1$. However, to the left of the point where the $\nu = 0$ curve reaches the horizontal axis, $V = 0$ is not a legitimate solution of the cutoff equation. The d/a value at which the $\nu = 0$ curve touches the horizontal axis is given by (31). This phenomenon finds the following simple explanation (private communication from E. A. J. Marcatili). As the mode approaches its cutoff value, we have $\gamma = 0$, and also $\theta = 0$, and $V = 0$. There is no longer any transverse field variation so that the field "senses" only the average value $\bar{n}^2$ of the dielectric constant of the tube,

$$\bar{n}^2 = \frac{\pi b^2 n_3^2 + \pi(a^2 - b^2)n_1^2}{\pi a^2}. \tag{34}$$

The mode is no longer guided if the average dielectric constant $\bar{n}^2$ is

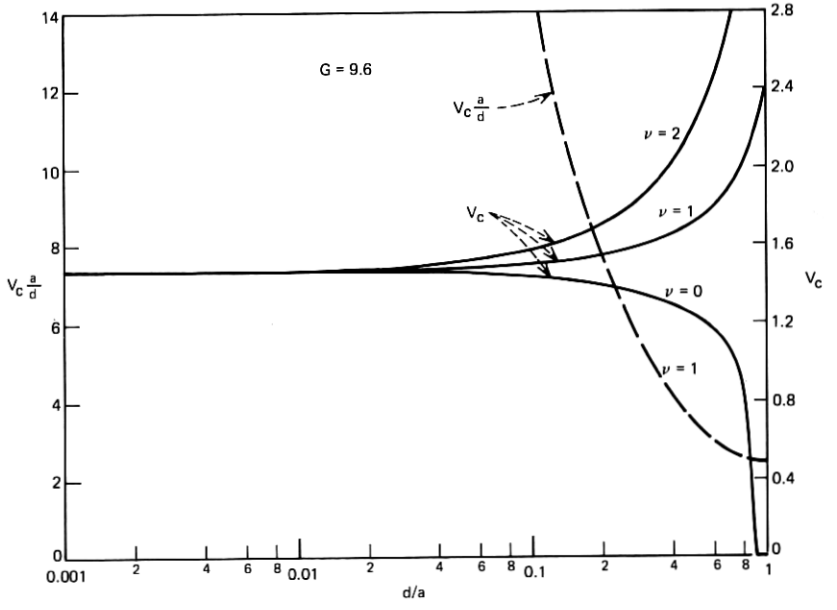

Fig. 6—Same as Fig. 3, $G = 9.6$.

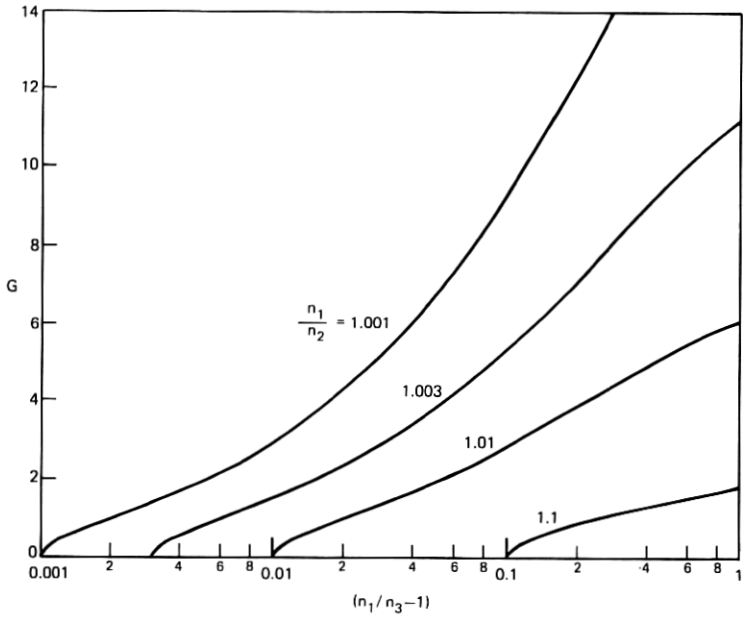

Fig. 7—The parameter G is shown as a function of $(n_1/n_3 - 1)$ for several values of n_1/n_2.

equal to the dielectric constants n_2^2 of the outer medium. The condition $\bar{n}^2 = n_2^2$ also leads to (31).

Figures 2 through 6 show that the cutoff points for all three modes ($\nu = 0$, 1, and 2) approach each other arbitrarily closely for small values of d/a. It is thus apparent that single-mode operation in the mode $\nu = 0$ becomes increasingly more difficult to achieve as the ratio d/a is decreased.

Finally, Fig. 8 shows a plot of the transverse decay parameter γa as a function of d/a. The curve is intended to provide information about single-mode operation of the tube waveguide. However, since it is desirable to operate with a tightly guided mode field, we chose as the operating point for V the cutoff value of the second mode, $V = V_{c1}$. It is a remarkable feature of the curves of Fig. 8 that they become independent of d/a for small values of this ratio. However, from the point of view of field confinement, we must remember that it is not γa but rather γd that characterizes the rate at which the field decays from the guiding structure–the tube–in radial direction. The crosses on the curves in Fig. 8 indicate the points at which we have $\gamma d = 1$, the circles indicate the points $\gamma d = 0.5$.

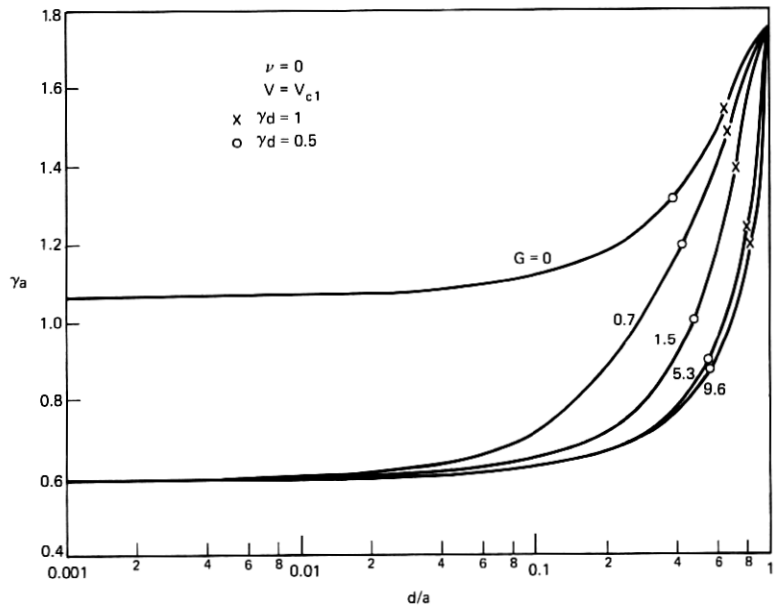

Fig. 8—This figure shows the parameter γa as a function of d/a for several values of G. V is taken equal to the cutoff value V_{c1} of the mode $\nu = 1$.

IV. CONCLUSIONS

The eigenvalue equation for the modes of the tube waveguide has been derived with the help of an approximate technique. The cutoff values of the normalized frequency parameter V [defined by (29)] are presented for the first three modes of the tube waveguide and the transverse decay parameter γa is plotted for the lowest-order mode under the assumption that this mode is operated at the point of cutoff of the next-higher-order mode.

One may wonder if it is possible to use the tube waveguide with single-mode operation to increase the mode radius compared to the mode radius of the lowest-order HE_{11} mode of the conventional fiber. This question has been studied under the assumption that both waveguides provide an equal amount of field confinement. The criterion for field confinement is the radial decay parameter γ. It was consequently assumed that the γ values of both waveguides are identical. Surprisingly, it was found that under the condition of single-mode operation for each guide and the requirement of equal field confinement, the mode radius of the tube waveguide is only slightly (approximately 40 percent) larger than the radius of the HE_{11} mode of the optical

fiber. A large mode radius appears desirable from the point of view of alignment tolerances of fiber splices. With a large mode radius, the alignment of the waveguide centers would be less critical. The tube waveguide does not appear to offer a significant advantage for this purpose.

REFERENCES

1. Kapron, F. P., Keck, D. B., and Maurer, R. D., "Radiation Losses in Glass Optical Waveguides," Appl. Phys. Ltrs., *17*, No. 10 (November 15, 1970), pp. 423–425.
2. Stone, J., "Optical Transmission Loss in Liquid-Core, Hollow Fibers," Conference on Integrated Optics-Guided Waves, Materials, and Devices, Optical Society of America, Digest of Technical Papers, pp. WA5-1–WA5-4.
3. Stone, J., "Optical Transmission in Liquid-Core Quartz Fibers," Appl. Phys. Ltrs., *20*, No. 7 (April 1972), pp. 239–240.
4. Beam, R. E., Astrahan, M. M., Jakes, W. C., Wachowski, H. M., and Firestone, W. L., "Dielectric Tube Waveguides," Final Report on Investigation of Multi-Mode Propagation in Waveguides and Microwave Optics, Microwave Laboratory, Northwestern University, Evanston, Illinois, May 1, 1949–November 30, 1950.
5. Kharadly, M. M. Z., and Lewis, J. E., "Properties of Dielectric-Tube Waveguides," Proc. IEEE, *116*, No. 2 (February 1969), pp. 214–224.
6. Snyder, A. W., "Asymptotic Expressions for Eigenfunctions and Eigenvalues of a Dielectric or Optical Waveguide," IEEE Trans. Microwave Theory Techniques, *MTT-17*, No. 12 (December 1969), pp. 1130–1138.
7. Gloge, D., "Weakly Guiding Fibers," Appl. Opt., *10*, No. 10 (October 1971), pp. 2252–2258.
8. Marcuse, D., *Light Transmission Optics*, New York: Van Nostrand Reinhold Company, 1972.
9. Jahnke, E., and Emde, F., *Tables of Functions with Formulas and Curves*, 4th Edition, New York: Dover Publications, 1945.
10. Grandshteyn, I. S., and Ryzhik, I. M., *Tables of Integrals, Series and Products*, 4th Edition, New York: Academic Press, 1965.